Int. J. Electrochem. Sci., 3 **(2008)** 908 - 917

International Journal of ELECTROCHEMICAL SCIENCE
www.electrochemsci.org

Electrochemical Characterization of Ni-Mo-Fe Composite Film in Alkali Solution

M. Jayalakshmi[1,*], *Woo-Young Kim*[2], *Kwang-Deog Jung*[2], *Oh-Shim Joo*[2]

[1] Non-ferrous Materials Technology Development Centre (NFTDC), Kanchanbagh, Hyderabad- 500 058, India.
[2] Hydrogen energy Research Centre, Korea Institute of Science and Technology (KIST), P.O. Box No.131, Chongryang, Seoul, S. Korea 130-650.
[*]E-mail: jayalakshmi@nftdc.res.in

Received: 23 April 2008 / *Accepted:* 12 May 2008 / *Online Published:* 30 June 2008

A composite Ni-Mo-Fe film galvanostatically coated on stainless steel substrate is studied for its electrochemical behavior in alkali solutions. The film is characterized by SEM-EDAX, ICP-AES, linear scan voltammetry and open-circuit potential decay transients. The main aim of this investigation is analyse the ternary metal coated film for its suitability as catalyst to water electrolysis. It is found that the film acts as a very good catalyst for hydrogen evolution in dilute alkali solution.

Keywords: Ni-Mo-Fe composite film; Stainless steel substrate; Galvanostatic deposition; Linear scan voltammetry; Catalytic behavior

1. INTRODUCTION

Nickel based electrode materials have been tried to produce hydrogen by water electrolysis that has attracted a rejuvenated interest due to recognition arising from the fact that hydrogen would be the fuel of the future. The recent development of combinatorial methods provides tools to speed the discovery process when a large number of candidate materials need to be synthesized and screened for the property of interest [1]. Combinatorial methods have been applied to optimize oxide materials for use as phosphors [2-5], gate dielectrics [[6] and fuel cell catalysts [7, 8]. The MacFarland group has demonstrated the electrochemical deposition of metal oxide compositions using robotics to plate and screen individually created materials and has looked at water photooxidation catalysts using multiplexed photoelectrochemical cells [9]. Electrodeposition is proved to be a cost-effective and non-equipment-intensive method for the preparation of nanophase and nanaocrystalline metallic materials. Moreover, nanoelectrodeposition has been recognized as a preparation method characterized by a

remarkable degree of reproducibility [10]. Catalytic materials are developed to minimize the over-voltages associated with hydrogen and oxygen gas evolutions so that high energy consumption for the process can be avoided.

To solve this problem, nickel based composite electrodes have been electrodeposited on stainless steel or copper substrates and studied for application as cathodes for industrial electrochemical production for hydrogen. Composite coated Raney nickel and thermally coated Ni/Mo coating electrodes were shown to exhibit higher electrocatalytic activities for hydrogen evolution reaction (HER) in alkaline solution but they were deactivated after two weeks due to power interruptions [11-13]. Ni based binary composite coatings like Ni-Mo, Ni-Zn, Ni-Co, Ni-W, Ni-Fe and Ni-Cr were tried for hydrogen electrodes; out of these electrodes, Ni-Mo was found to be best and most stable electrode with an overpotential of 0.18 V in 6 M KOH solutions [14]. A series of ternary Ni composites such as Ni-Mo-Fe, Ni-Mo-Cu, Ni-Mo-Zn, Ni-Mo-W, Ni-Mo-Co and Ni-Mo-Cr were studied for hydrogen evolution and the authors reported that the best and most stable cathode was Ni-Mo-Fe [15-17]. High stability of amorphous Ni-Mo-Fe electrode was confirmed by other authors who tested the electrode with current interruptions [18]. Recently, electrodeposited cathode coatings like Ni-S, Ni-Mo, Ni-Ti, Ni-Mo-Si, and Ni-Fe-Mo-Zn were tailored and studied for hydrogen production [19-26]. Addition of cobalt was shown to improve the electrocatalytic property for oxygen evolution while the sulphur added helps to activate the hydrogen evolution in alkali solutions [27-29]. Alloying nickel with left transition metals (W, Mo and Fe) was shown to increase the intrinsic electrocatalytic activity in the HER compared to pure nickel [30]. The combined effect of these metals was explained by a synergy model which is based on the known dynamics of adsorbed hydrogen over such metals together with demonstrable electrocatalytic behavior [31].

It is well established that that Pt metal is the best electrocatalyst for hydrogen evolution as the reaction in essence is thermoneutral i.e the rate of adsorption of protons on the surface is almost equal to the rate of desorption or recombination to form hydrogen gas (ΔG = -0.1 eV). Next ideal metal is Ni (ΔG = -0.28 eV) followed by Mo (ΔG = -0.36 eV) [32]. In our recent work, we reported the effect of substrates like Pt/Si, graphite, steel, nickel and stainless steel on the electrochemical behavior of Ni-Mo-Fe-Co-S composite film in alkali solutions [33]. The present work deals with the preparation of Ni-Mo-Fe ternary film on stainless steel substrate by galvanostatic deposition and its electrochemical characterization in alkali solutions. The ternary film was characterized by SEM, EDAX and ICP-AES analysis. Linear scan voltammetry was done in 0.1 to 5 M NaOH alkali solutions in order to determine the catalytic potentials for hydrogen and oxygen evolutions. Open-circuit decay transients were also recorded to understand the corrosion behavior.

2. EXPERIMENTAL PART

2.1. Electrodeposition of Ni-Mo-Fe film

The films were galvanostatically deposited on stainless steel substrates by applying a constant current of 900 mA (450 mA/cm^2) for a period of 10 minutes. The geometric area exposed for coating

was 1 cm^2 on each side (2 cm^2 in total). The composition of the plating bath was as follows: $NiSO_4.7H_2O$ (6.5 g/l); $NiCl_2$ (3.5 g/l); Na_2MoO_4. $2H_2O$ (1.0 g/l); $FeSO_4.7H_2O$ (1.0 g/l); $K_3C_6H_5O_7.H_2O$ (6.0 g/l); $(NH_4)_2CO$ (8.0 g/l). The pH of the plating solution was 7 and the deposition was carried out at room temperature (298 K) with continuous stirring.

2.2. Characterization

The film composition was determined by ICP-AES (inductively coupled plasma –atomic emission spectroscopy) in a Prodigy high dispersion model, Leeman laboratory Inc. The semi-quantitative elemental composition of the film was determined using energy dispersive X-ray (EDAX) analysis using horida-ex-200, Japan, with spatial resolution of 134 eV. Surface morphological studies were carried out with scanning electron micrographs, obtained with FE-SEM, (SM-6340 F, Jeol, Japan). Linear scan voltammograms (LSVs) and open-circuit potential decay measurements were carried out in a conventional three electrode assembly using a potentiostat/galvanostat (EG&G Princeton Applied Research, Model 273A) interfaced with a computer. An Ag/AgCl electrode was used as the reference electrode and a large Pt foil was employed as the counter electrode.

3. RESULTS AND DISCUSSION

3.1. SEM images

Thickness of Ni-Mo-Fe films was in the range of 13.2 to 17.6 μm. The films were amorphous as the thin film XRD could not identify any peaks pertaining to the three co-deposited metals. The SEM image of the ternary film with spherical, well-formed particles ranging from 130 to 270 nm was shown in Fig. 1. The film was highly porous with a cloud of nanometric particles of varying sizes and uniform shapes touching each other with free spaces lingering between them.

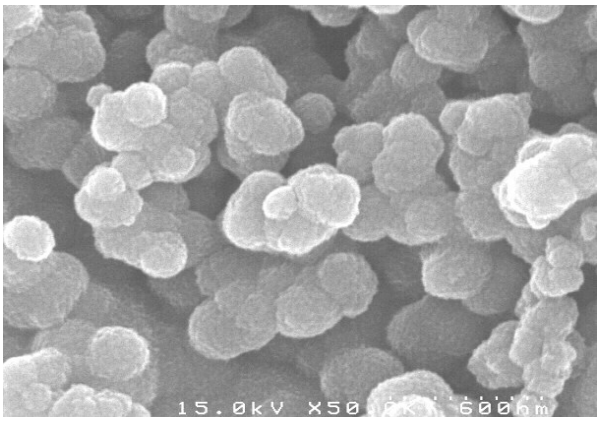

Figure 1. SEM image of Ni-Mo-Fe composite film coated on stainless steel substrate

3.2. Film composition

The composition of the Ni-Mo-Fe film determined by ICP-AES analysis was as follows: Ni, 10.1; Mo, 1.79; Fe, 1.0 and EDAX analysis of the same film gave the following composition: Ni, 9.09; Mo, 1.25; Fe, 1.92 (Fig. 2).

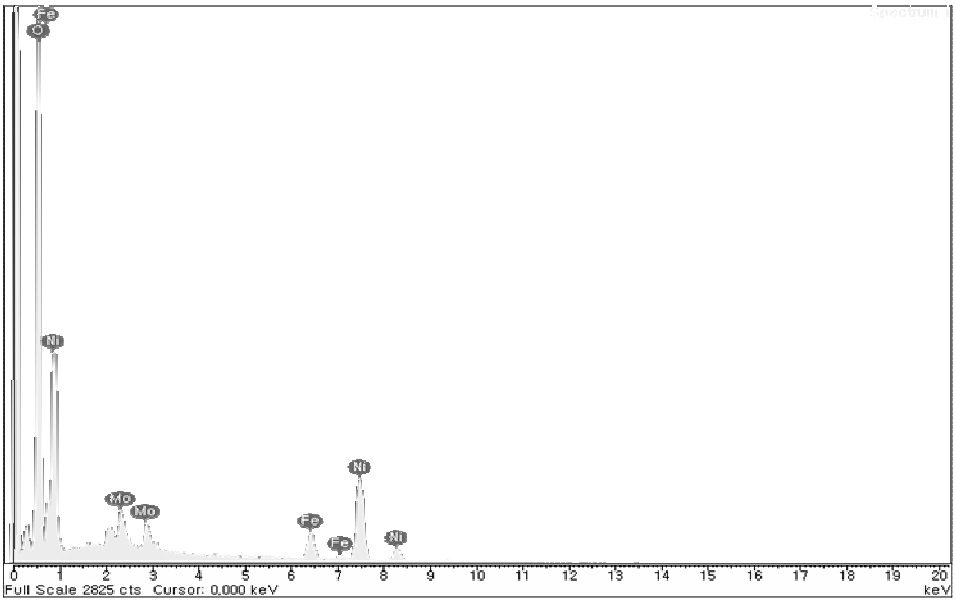

Figure 2. EDAX image of Ni-Mo-Fe composite film

3.3 Electrochemical studies

3.3.1. Linear scan voltammetric studies

Fig. 1 shows the linear scan voltammgorams (LSVs) recorded for the Ni-Mo-Fe ternary film in the NaOH solutions varying from 0.1 to 5.0 M. The idea of using LSVs as a screening tool to determine the oxygen and hydrogen gas evolutions in electrode surfaces made of totally new materials is borrowed from phtotoelectrochemical cells; for an electrode to work ideally for photosplitting, the difference in redox onset potentials of the oxygen and hydrogen evolutions (E_O-E_H = ΔE) represents E_g^{LSV} which is termed as electrochemical bandgap. Here the anodic and cathodic onset potentials are basically related to the exhaustion of available sites for the adsorbed species. LSVs, on the other hand give the onset potentials of the oxygen and hydrogen evolutions as well as the overpotentials which are highly relevant in conventional water electrolysis. The onset potentials were noted from the rising portion of the curves in Fig. 3, as the gas evolution is usually indicated by a sharp rise in current either in positive or negative direction. Table 2 presents these values for hydrogen and oxygen evolution in all the alkali concentrations.

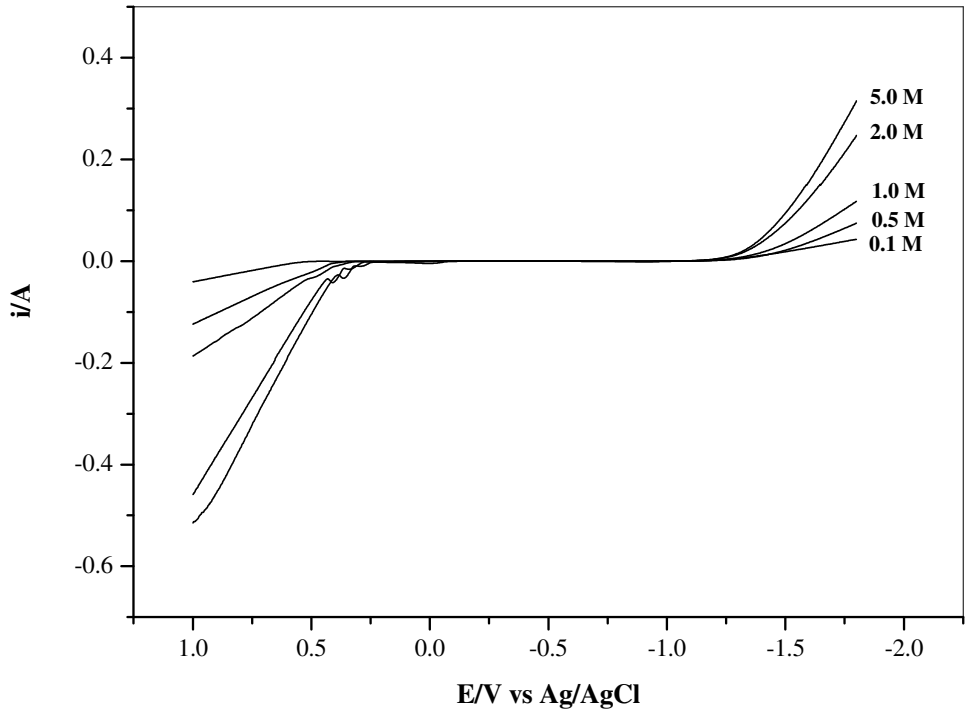

Figure 3. Linear scan voltammograms of Ni-Mo-Fe film coated on stainless steel substrate in 0.1- 5.0 M NaOH solutions; scan rate = 50 mVs^{-1}.

Prior to the discussion pertaining to the overpotentials of these gas evolutions in the presence of ternary film, it is necessary to determine the theoretical potentials at which the both gas evolutions can possibly occur in the varying alkali concentrations. This exercise is quite important as the pH varies with the alkali concentration and it has a telling effect on the potentials. The theoretical values for E_O and E_H are calculated using the following equations derived from Nernst law as [34]:

Hydrogen electrode: $2H^+ + 2e \longrightarrow H_2\uparrow$

Nernst equation for this reaction is,

$E_{H_2} = E^o + 0.059/n \log [a_{H+}]^2$ (Partial pressure of hydrogen =1)

$= E^o + 0.059/2 \times 2x - pH$ ($pH = \log a_{H+}$, $E^o = 0$)

$= -0.059 \times pH$

Oxygen electrode: $2H_2O + O_2 + 4e = 4 OH^-$

$E_{O_2} = E^o + 0.059/n \log P_{O_2} / [a_{OH-}]^2$ ($E^o = 0.401$ V)

$= 0.401 - 0.059 \times pOH$

Table 1. Theortical hydrogen and oxygen evolution potentials determined from the Nernst law for varying alkali concetrations

NaOH (M)	pH	Rev. hydrogen electrode potential (V vs. Ag/AgCl)	Rev. oxygen electrode potential (V vs. Ag/AgCl)
0.1	13.0	-0.992	0.541
0.5	13.7	-1.033	0.582
1.0	14.0	-1.051	0.600
2.0	14.3	-1.069	0.618
5.0	14.7	-1.092	0.640

Table 2. Hydrogen and oxygen evolution (onset) potentials determined from the LSVs for varying alkali concentrations

NaOH (M)	Hydrogen evolution		Oxygen evolution	
	Onset pot. (V)	Over pot. (V)	Onset Pot. (V)	Under pot. (V)
0.1	-1.060	0.068	0.500	0.041
0.5	-1.120	0.087	0.375	0.207
1.0	-1.170	0.119	0.270	0.330
2.0	-1.256	0.187	0.310	0.308
5.0	-1.310	0.218	0.260	0.380

The values obtained are in SHE scale and has to be converted to Ag/AgCl reference scale so that comparison with the experimental values is reasonable. Table 1 shows the reversible gas evolution potentials in Ag/AgCl scale. It could be seen from Table 1, the onset potential for H_2 evolution shifts towards negative direction whereas the onset potential for O_2 evolution shifts towards positive direction with increase in alkali concentrations. These values do not reflect the electrodics but reflect the change of potential with the change in ratio of anions and cations.

The logic in deciding the overpotential for the gas evolutions may be explained as follows: if an electrode/electrolyte interface is assumed to be in equilibrium, then the rate of oxidation is equal to rate of reduction. In such a situation, the net flow of current across the interface would be zero. Underlying the conditions of zero net current, equilibrium exchange current density (i_o) flows across

the interfaces in both direction. The potential difference across the interface ($\Delta\varphi$) at equilibrium depends upon the activity ratio of anions and cations in the solution. During the passage of external current or voltage to drive a reaction, interfaces move away from the equilibrium so that a potential difference corresponding to that magnitude is produced (Galvani potential difference $\Delta\varphi_e$). Then the current density 'i' across the interface is linked to the overpotential or excess potential, $\eta = \Delta\varphi - \Delta\varphi_e$. In a driven electrochemical system, it is the excess potential difference that drives the current density. This means that increase in net oxidation current density would result in an excess potential at the electron-sink electrode (anode) to be more positive ($\Delta\varphi > \Delta\varphi_e$). Similarly, an increase in net reduction density would result in a $\eta = \Delta\varphi - \Delta\varphi_e$ where $\Delta\varphi < \Delta\varphi_e$ so that the excess potential at the electron-reservoir electrode (cathode) would be more negative [34].

The role of catalyst is to reduce the current density by lowering the activation energy barrier so that the magntitude of overpotentials shall be reduced. In our earlier work, we reported the electrocatalytic behavior of electroless NiP coated on graphite in alkali/dextrose solutions; the catalytic effect was identified by the shift of potentials in the positive direction for the anodic reaction and negative direction for the cathodic reaction with the increase in dextrose concentrations; the shift of anodic potential toward positive direction is attributed to the nickel oxide film formation on the electrode surface [35]. In the present work, Table 2 presents the onset potentials noted from the LSV curves in Fig. 3 for both gas evolutions. The overpotentials for hydrogen and oxygen evolutions are calculated from the difference between the theortical (Table 1) and experimental values. The onset potentials for hydrogen evolution shift towards negative direction whereas that of oxygen evolution also shifts towards negative direction. Very low overpotential for both gas evolutions are observed in dilute 0.1 M NaOH solution. The difference in potentials of both gas evolutions i.e the voltage window, an essential criteria for water electrolysis is also minimum in 0.1 M NaOH solution. Hence the ternary Ni-Mo-Fe film use as catalytic film for water electrolysis is highly feasible in dilute alkali solutions.

3.3.2. Open-circuit potential decay transients

Open-circuit potential decay (OCP) transients have been measured to understand the processes which occur after switching off the charging current. This method of recording decay of potential (potential relaxation) on open-circuit following interruption of a polarizing current of an electrode reaction, provides data leading to information on the interfacial capacitance behavior of the electrode. In cases of hydrogen evolution reactions, where steady-state coverage by adsorbed intermediates is quite large, an adsorption pseudocapacitance is generated. The OCP decay transients as against the cyclic voltammetric method, enables to determine the pseudo double layer capacitance over an appreciable range of overpotentials where substantial Faradic currents for the reaction were previously passing [36, 37]. Tilak and Convey gave a simple equation for this potential relaxation behavior as,

$$-C\, dE/dt = i_f$$

Under open-circuit conditions where $i_f = 0$, dE/dt values derived from the OCP transients are a measure of double layer capacitance (C); it is known that C reflects the changes in charges in the Helmholtz inner layer. The Ni-Mo-Fe thin films were charged cathodically by applying various currents for 120 seconds. Fig. 4 shows the OCP decay transients obtained for hydrogen evolution in 5.0 M NaOH solution and Table 3 shows the parameters derived from the curves. As soon as the current was switched off, the change in potential of the Ni-Mo-Fe electrode with time was noted. The fall in potential was rapid in the initial 50 seconds and then the electrode potential gets stabilized. One could see the OCP shifts in the negative direction with increase in current densities. Application of cathodic current would enable the adsorption of anions at the metal/solution interface, while the electroneutrality requires that the increase in charge of the particles due to electrons will be balanced by a corresponding increase in positive ion charge (protons) and the eventual desorption of protons as hydrogen gas occurs. In the OCP conditions, the anions would remain adsorbed to the electrode surface in the inner Helmholtz layer; the extent of anion adsorption being directly proportional to the magnitude of current applied. This was responsible for the OCP values being shifted towards negative direction with increase in applied current densities. This condition is similar to that of a semiconductor where the band edge alignment depend on the accumulation of charges at the interface in which case, the adsorption of positive ions would shift the band edge (CB) towards positive direction; on the reverse negative scan, the adsorption of negative ions would shift the band edges (VB) towards negative direction [38, 39].

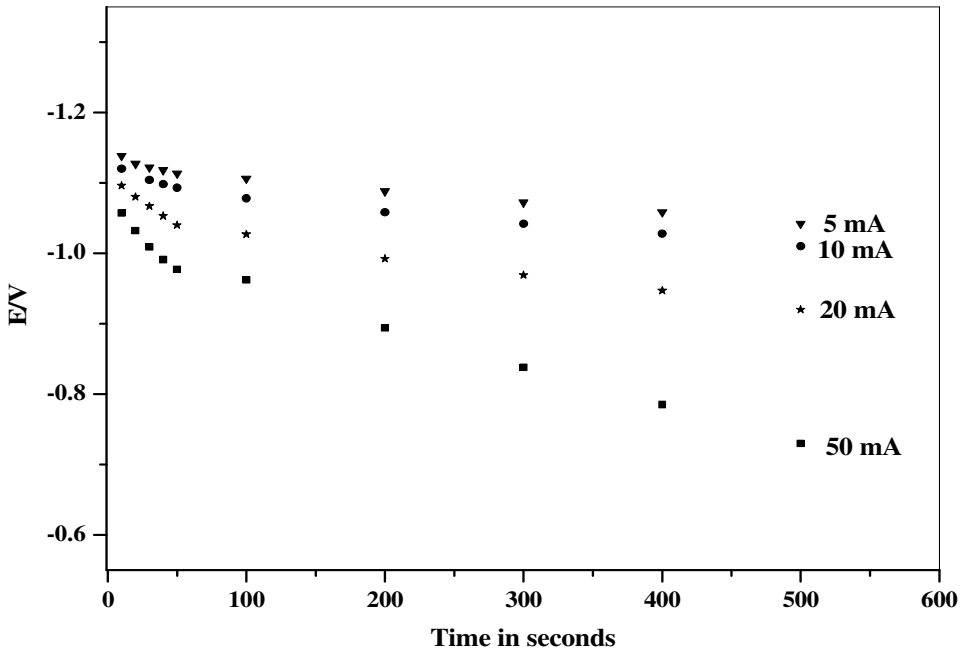

Figure 4. Typical OCP decay curves of Ni-Mo-Fe film at various applied cathodic currents

4. CONCLUSIONS

Ternary Ni-Mo-Fe film coated on stainless steel substrate was found to be catalytic to hydrogen evolution in dilute alkali solutions. The overpotentials for both hydrogen and oxygen evolutions were minimum in 0.1 M NaOH solution. The potential window between the oxygen and hydrogen evolutions was the lowest in 0.1 M NaOH solution which is highly desired for water electrolysis.

ACKNOWLEDGEMENTS
This research was performed for the Hydrogen Energy R&D Center, one of the 21st Century Frontier R&D program, funded by the Ministry of Science and Technology of Korea. One of the authors, (MJ) wishes to thank the Korean Federation of Science and Technology Societies (KOFST), Korea for award of Brain Pool Fellowship (2006-2007).

References

1. E. Reddington, A. Sapienza, B. Gurau, R. Viswanathan, S. Sarangapeni, E. S. Smotkin, T. E. Mallouk, *Science*, 280 (1998) 1735
2. J. Wang, Y. Yoo, C. Gao, I. Takeuchi, X. Sun, H. Chang, X.-D. Xiang, P. G. Schultz, *Science,* 279 (1998) 1712
3. X. -D. Sun, C. Gao, J. Wang, X. -D. Xiang, *Appl. Phys. Lett.* 70 (1997) 3353
4. E. Danielson, M. Devenney, D. M. Giaquinta, J. H. Golden, R. C. Haushalter, E. W. McFarland, D. M. Poojary, C. M. Reaves, W. H. Weinberg, X. D. Wu, *Science,* 279(1998) 837
5. E. Danielson, J. H. Golden, E. W. McFarland, C. M. Reaves, W. H. Weinberg, X. D. Wu, *Nature,* 389 (1997) 944
6. R. B. Dover, L. F. Schneemeyer, R. M. Fleming, *Nature,* 392 (1998) 162
7. T. J. Jaramillo, A. Ivanovskaya, E. W. McFarland, *J. Comb. Chem.* 4 (2002) 17
8. P. Cong, R. D. Doolen, Q. Fan, D. M. Giaquinta, S. Guan, E. W. McFarland, D. Poojary, K. Self, H. W. Turner, W. H. Weinberg, *Angew. Chem., Int. Ed.* 38 (1999) 484
9. S. H. Baeck, T. F. Jaramillo, C. Brandli, E. W. McFarland, *J. Comb. Chem.* 4 (2002)563
10. L. P. Bicelli, B. Bozzini, C. Mele, L. D'Urzo, *Int. J. Electrochem. Sci. 3 (2008)356.*
11. E. Endoh, H. Otouma, T. Morimoto, Y. Oda, *Int. J. Hydrogen Energy*, 12 (1987) 473
12. Y. Choquette, H. Menard, L. Brossard, *Int. J. Hydrogen Energy*, 14 (1989) 637
13. I. Arul Raj, V. K. Venkatesan, *Int. J. Hydrogen Energy*, 13 (1988) 215
14. I. Arul Raj, K. I. Vasu, *J. Appl. Electrochem*. 20 (1990) 32
15. I. Arul Raj, *Int. J. Hydrogen Energy*, 17 (1992) 413
16. I. Arul Raj, *Appl. Surface Sci*. 59 (1992) 245
17. I. Arul Raj, *J. Appl. Electrochem*. 22 (1992) 471
18. W. Hu, Y. Zhang, D. Song, Z. Zhou, Y. Wang, *Mater. Chem. Phys*. 41 (1995) 141
19. Q. Han, K. Liu, J. Chen, X. Wei, *Int. J. Hydrogen Energy,* 28 (2003) 1207
20. H. He, H. Liu, F. Liu, K. Zhou, *Mater. Lett*. 59 (2005) 3968
21. L. S. Sanches, S. H. Domingues, C. E. B. Marino, L. H. Mascaro, *Electrochem. Commun.* 6 (2004) 543
22. J. Panek, A. Serek, A. Budniok, E. Rówinski, E. Lagiewka, *Int. J. Hydrogen Energy*, 28 (2003) 169
23. J. Kubisztal, A. Budniok, *Appl. Surface Sci.* 252 (2006) 8605
24. J. Kubisztal, A. Budniok, A. Lasia, *Int. J. Hydrogen Energy*, 32 (2007) 1211
25. M. Kubisztal, J. Kubisztal, A. Chrobak, G. Haneczok, A. Budniok, J. Rosek, *Surf. Coat. Technol.* (2007)-in press doi:10.1016/j.surfcoat.2007.07.057

26. F. C. Crnkovic, S. A. S. Machado, L. A. Avaca, *Int. J. Hydrogen Energy,* 29 (2004) 249
27. Y. Zhang, X. Cao, H.Yuan, W. Zhang, Z. Zhou, *Int. J. Hydrogen Energy,* 24 (1999) 529
28. M. Isabel Godinho, M. Alice Catarino, M. I. da Silva Pereira, M. H. Mendonc,F. M. Costa, *Electrochim. Acta*, 47 (2002) 4307
29. M. Jayalakshmi, V. S. Muralidharan, *Br. Corrosion J*. 26 (1991) 123.
30. E. Navarro-Flores, Z. Chong, S. Omanovic, *J. Mol. Catal. A: Chem*. 226 (2005) 179
31. J. G. Highfield, E. Claude, K. Oguro, *Electrochim. Acta*, 44 (1999) 2805
32. H. Deng, I. Ishikawa, M. Yoneya, H. Nanjo, *J. Phys. Chem*. 108 (2004) 9138
33. M. Jayalakshmi, Indra Puspitasari, Kwang-Deog Jung, Oh-Shim Joo, *Int. J. Electrochemical. Sci*. 3 (2008) 787.
34. J. O' M. Bockris, A. K. N. Reddy, M. Gamboa-Aldeco, 'Fundamentals of Electrodics- Modern Electrochemistry 2A,' Second Edition, Springer, N.Y. 2006.
35. G. Veera Babu, M. Palaniappa, M. Jayalakshmi, K. Balasubramanian, *J. Solid State Electrochem.* 11(2007) 1705
36. B.V. Tilak, B.E. Conway, *Electrochim. Acta*, 21 (1976) 745
37. B.V. Tilak, C.G. Rader, BE. Conway, *Electrochim. Acta*, 22 (1977) 1167
38. M. Batzill, E.L.D. Hebenstreit, W. Hebenstreit, U. Diebold, *Chem. Phys. Lett*. 367 (2003) 319.
39. S. R. Morrison (Ed.), Electrochemistry at Semiconductor and Oxidized Metal Electrodes, Plenum Press, New York, 1980, p. 62